

Recent Developments in Gravitational Microlensing

Andrew Gould

Ohio State University

Abstract. Twenty-one years after Bohdan's seminal paper launched the field of gravitational microlensing, it has radically diversified from a method narrowly focused on finding dark matter to a very general astronomical tool. Microlensing has now detected 12 planets, including several that are inaccessible by other search methods. It has resolved the surfaces of distant stars, served as a magnifying glass to take spectra of extremely faint objects, and revealed a number of surprising phenomena. I take a sweeping look at this remarkable technique, giving equal weight to its successes and to the tensions that are continuing to propel it forward.

1. Introduction

While the idea of microlensing goes back to the famous Einstein (1936) paper in *Science*, and is worked out in even greater detail in Einstein's notebooks from 1912 (Renn et al. 1997), Bohdan Paczyński (1986) was the first to recognize that with the arrival of modern CCDs and the high-speed computing required to analyze them, microlensing's time had come.

The focus of Bohdan's original paper on this subject was dark matter, and it prompted two major surveys toward the Large Magellanic Cloud (LMC), which are reviewed by Charles Alcock in this volume. But Bohdan was always looking to push microlensing in new directions, most notably in his two seminal papers that launched microlensing studies of Galactic structure (Paczynski 1991) and microlensing planet searches (Mao & Paczyński 1991). Over the past 15 years, microlensing has developed as an important tool in both these areas, and a third area as well: stellar atmospheres.

Parallel to this broad invasion of several areas of astrophysics, microlensing activists pushed the field in a number of narrow, rather arcane, directions, exploring weird higher-order effects such as those due to finite source size, orbital parallax, terrestrial parallax, xallarap, lens rotation, as well as degenerate solutions, and microlensed variables. One of the most exciting and unexpected developments in microlensing has been that these weird effects, originally of interest only to microlensing nerds, have started to interpenetrate with the more mainstream investigations outlined in the previous paragraph. This is because they provide additional information that is of interest to a more general astronomical audience and make microlensing applications more powerful.

In this contribution, I review some of these developments, pointing to these interconnections whenever possible.

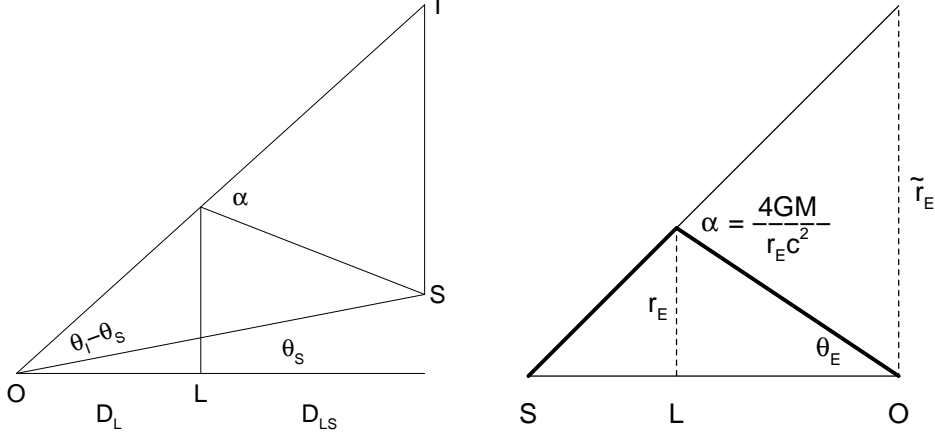


Figure 1. Left: Point-lens microlensing. Mass (M) deflects light from source (S) by Einstein bending angle $\alpha = 4GM/(c^2 D_L \theta_I)$ to observer (O). Right: Relation of higher-order observables, the angular (θ_E) and projected (\tilde{r}_E) Einstein radii, to physical characteristics of the lensing system. Adapted from Gould (2000).

2. Microlensing Basics

It is a mark of the simplicity of point-lens microlensing that the basic results, including the main higher-order effects, can be encapsulated in two simple diagrams (Fig. 1) and a few simple equations.

Equating (from Fig. 1a) $\overline{IS} = \alpha D_{LS} = (\theta_I - \theta_S) D_S$, where $D_S = D_L + D_{LS}$, yields the quadratic equation, $\theta_I(\theta_I - \theta_S) = \theta_E^2$, which sets the fundamental Einstein angular scale $\theta_E^2 \equiv (4GM/c^2)(D_L^{-1} - D_S^{-1})$. The two solutions are $u_{\pm} = (u \pm \sqrt{u^2 + 4})/2$, where $u \equiv \theta_S/\theta_E$ and $u_{\pm} \equiv \theta_{I\pm}/\theta_E$ are scaled to θ_E . Because surface brightness is conserved, the magnification A is given by the ratio of the combined area of the images to the area of the source:

$$A_{\pm} = \left| \frac{u_{\pm}}{u} \frac{du_{\pm}}{du} \right|, \quad A = A_+ + A_- = \frac{u^2 + 2}{u\sqrt{u^2 + 4}}. \quad (1)$$

The two higher-order observables shown in Figure 1b, the angular (θ_E) and projected (\tilde{r}_E) Einstein radii, can be measured if the event can be compared to standard rulers on the sky and observer planes, respectively. See § 5. These are then easily related to the mass M and the source-lens relative parallax $\pi_{\text{rel}} = \text{AU}(D_L^{-1} - D_S^{-1})$. First, $\alpha/\tilde{r}_E = \theta_E/r_E$, so $\theta_E \tilde{r}_E = \alpha r_E = 4GM/c^2$. Next, by the exterior angle theorem, $\theta_E = \tilde{r}_E/D_L - \tilde{r}_E/D_S = (\tilde{r}_E/\text{AU})\pi_{\text{rel}}$. In summary,

$$M = \frac{\theta_E}{\kappa\pi_E}, \quad \pi_{\text{rel}} = \theta_E\pi_E, \quad \theta_E = \sqrt{\kappa M\pi_{\text{rel}}}, \quad \pi_E = \sqrt{\frac{\pi_{\text{rel}}}{\kappa M}}, \quad (2)$$

where $\kappa \equiv 4GM/(c^2\text{AU}) \sim 8.14 \text{ mas } M_{\odot}^{-1}$ and $\pi_{\text{E}} \equiv \text{AU}/\tilde{r}_{\text{E}}$.

3. Microlensing Planet Searches

Mao & Paczyński (1991) showed that if a lens had a companion, it would distort the primary lens’s magnification field, inducing an “astigmatism” or “caustic structure” near the peak. These caustics are closed contours of formally infinite magnification (see, e.g., Fig. 2a, below): the magnification diverges according to a square-root singularity as the source approaches the caustic from the inside. The bigger the companion, the bigger the caustic, and so the greater the chance that the source would pass close enough to the lens to be affected. But their main point was: even a planet could in principle be detected.

Of course, just as the planet perturbs the magnification pattern of its host, the host also perturbs the planet field. Since the host is much bigger than the planet, this perturbation is also much bigger, so a random source is much more likely to pass over the resulting “planetary caustic” than the “central caustic” highlighted by Mao & Paczyński (1991). This fact led Gould & Loeb (1992) to focus on planetary caustics the next year when we advocated a search+followup strategy for finding planets. Microlensing events are extremely rare (optical depth $\tau \sim 10^{-6}$), so huge areas must be surveyed each night, which limits the number of observations of each field. But since the planetary perturbations are extremely short $t_p \sim (M_{\text{planet}}/M_{\text{Jupiter}})^{1/2}$ day, the events that are found must be intensively monitored by other, “followup” telescopes scattered around the globe, in order to trace out the planetary signature.

Although hardly noticed at the time, this subtle difference in emphasis between these two papers grew into a major divergence, which has since dominated all issues connected with microlensing planet searches.

3.1. 1st Microlensing Planet – Pure-Survey Jupiter

In 1995, Penny Sackett formed the PLANET collaboration (Albrow et al. 1998) to carry out this survey+followup strategy, but it was not until 2003 that the first planet was discovered, OGLE-2003-BLG-235/MOA-2003-BLG-53Lb, and this was by the survey teams themselves, not the followup groups (Bond et al. 2004). Why? The event had a 7-day planetary deviation, so the nightly survey data were basically adequate to characterize it, which would not have been the case had it lasted just 1 day (or less), as expected. The perturbation was long because the planet was sitting right next to the Einstein ring, and so induced a big caustic. Such alignments are rare, but the survey groups are well poised to find them because they monitor of order 600 events per year. The followup groups, by contrast, monitor only the few dozen “most promising” events. The survey-group discovery of the first microlensing planet was the first piece of evidence that the survey+followup strategy originally advocated by Gould & Loeb (1992) would require radical rethinking if it were to be successful.

3.2. High-Magnification Events

In the meantime, Jaroszyński & Paczyński (2002) found a planet-candidate based on a single deviant point, which consequently could not be confirmed. This

prompted Andrzej Udalski (see these proceedings) to develop the OGLE “Early Early Warning System (EEWS)”, which would alert the OGLE observer when an already-identified event was behaving “unusually”, thereby enabling OGLE both to alert the community and to carry out “auto-followup” observations itself. This system actually went off on OGLE-2004-BLG-343, a spectacular magnification $A = 3000$ event, but unfortunately the alarm was ignored by the observer. However, Dong et al. (2006) showed that if this event had been properly monitored, it would have had excellent sensitivity to Earth-mass planets, and even some sensitivity to Mars-mass planets. That is, the “central caustic” (i.e. high-magnification) events originally highlighted by Mao & Paczyński (1991) were actually much better targets than the larger-caustic events singled out by Gould & Loeb (1992). Even though the caustics (and so the number of caustic-crossing events) are smaller, the events in which this happens can be identified *in advance*, enabling intensive followup right in the period of greatest sensitivity. Actually, this same point had previously been made by several theorists (Griest & Safizadeh 1998; Rattenbury et al. 2002), but as often happens, it was the practical demonstration that had the biggest impact.

Another, completely unrelated development, pushed the Microlensing Follow Up Network (μ FUN) in the direction of high-mag events. Jennie McCormick, a New Zealand amateur, sent me an email one day saying “I have data on your event, what do you want me to do with it?” Of course, it seemed preposterous that a 12” telescope in one of the wettest places in world could make a material contribution, but I started sending her our microlensing alerts. She contacted Grant Christie, another NZ amateur, who ultimately made contact with almost a dozen other amateurs around the southern hemisphere. As these amateurs had to work during the day, we had to limit requests to only the most sensitive events, generally high-mag events. Eventually, we realized that even at our professional-class telescopes, we were wasting our time following non-high-mag events. By 2005, our conversion was complete.

3.3. 2nd Microlensing Planet – High-Mag Jupiter

The first fruit of this new strategy came early the next year when OGLE-2005-BLG-071 started approaching high magnification. Both OGLE and μ FUN Chile intensively observed the event as it approached its peak until observations were cut off by dawn. Shortly thereafter, however, Jennie and Grant began observing on their 12” and 14” scopes (see Fig. 2a). Over four nights, OGLE and μ FUN telescopes traced out a triple-peak event: two big peaks flanking a small peak in the middle, implying that the source passed by a caustic with three cusps: strong, weak, strong (see lower inset to Fig. 2a). It can be proved mathematically that such a geometry can only be produced by a planet. Jennie’s comment: “It just shows that you can be a mother, you can work full time, and you can still go out there and find planets.”

3.4. 3rd Microlensing Planet – Survey+Followup Super-Earth

The PLANET collaboration has dedicated access to 4 1m-class telescopes for May–August. This caused them to miss OGLE-2005-BLG-071, which peaked in April, but enables them to follow many more events during the 4-month “high season”, i.e., not just the rich but rare high-mag events, but the run-of-the-mill

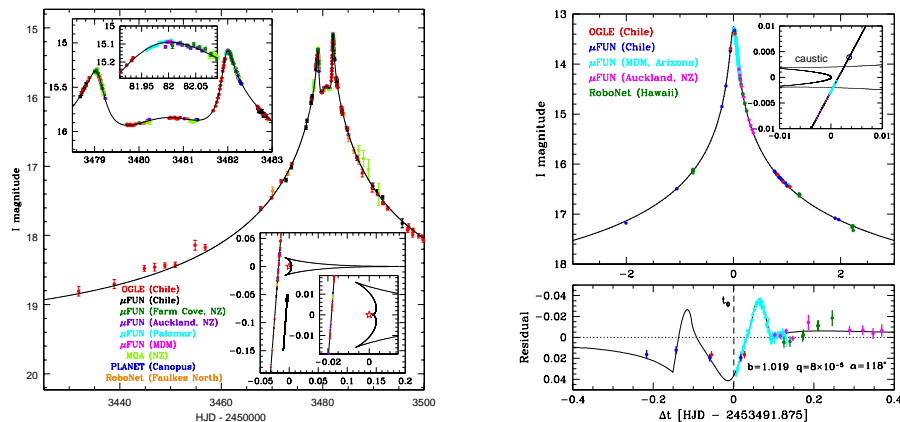


Figure 2. Left: Jupiter-mass planet in high-mag event OGLE-2005-BLG-071. Two major peaks and small peak in middle (upper inset) imply source passes by two major cusps and a weak cusp in between (lower inset). This caustic geometry can only be produced by planetary companions, in this case with mass ratio $q = 7 \times 10^{-3}$. From Udalski et al. (2005). Right: Neptune-mass planet in high-mag event OGLE-2005-BLG-169. Upper panel shows “basically normal” event, but residuals to point-lens fit reveal 2% deviations. Detailed modeling is required to uncover the caustic structure (inset) due to planet with $q = 8 \times 10^{-5}$, i.e. almost 100 times smaller than OGLE-2005-BLG-071. From Gould et al. (2006).

events originally advocated by Avi and me. One of these, OGLE-2005-BLG-390 showed a second bump well after peak. The rounded shape of this bump implies that its full duration, $2t_p \sim 0.6$ days is dominated by the size of the source rather than the caustic. This is expected because the source was very bright and red, hence very big. Under these conditions, it is straightforward to show that the planet/star mass ratio is approximately, $q = (A_p/2)(t_p/t_E)^2$, where A_p is the amplitude of the second bump and $t_E = 10$ days is the Einstein timescale. That is, one can simply read off the lightcurve, without any analysis, $q = 9 \times 10^{-5}$. In fact, detailed analysis (Beaulieu et al. 2006) yields $q = 8 \times 10^{-5}$, corresponding to 5.5 Earth masses at the estimated $M \sim 0.2 M_\odot$ mass of the host. This is also the first event for which both survey and followup were absolutely required. Both of the previous planets had perturbations lasting several days, which allowed them to be basically characterized from survey data alone, even though the followup data did substantially improve the characterization in the case of OGLE-2005-BLG-071Lb.

3.5. 4th Microlensing Planet – High-Mag Neptune

Just a week after OGLE-2005-BLG-071 subsided, another event was approaching peak, OGLE-2005-BLG-169. In this case, OGLE did not observe the event at all for 6 days before peak, the first 4 because of weather and the last 2 because the telescope was dedicated to Chilean observations. Based on “general suspicion” that it might become high-mag, μ FUN obtained some observations, but the night before peak, the case was still not convincing: μ FUN (i.e., AG) failed to pursue

the event aggressively, but did ask Andrzej (who was at the OGLE telescope, service observing for the Chileans) to sneak in an observation of this event. An email came back at 3 a.m.: the event was extremely high-mag and there were no observations being taken! I was asleep, but heard the “ping” of my email and went upstairs to have a look. I was quite dazed but eventually realized that the event could be observed over peak from MDM, despite its northern location. I called up the observer who happened to be an OSU grad student, Deokkeun An. I implored him to take time out of his own observing to obtain 9 images of this event over the next 3 hours. Recognizing that my request was much too timid, Deokkeun actually took over 1000 observations, which traced out a 2% deviation from a magnification $A = 800$ event (see Fig. 2b). As in a number of other microlensing events, the initiative of the observer proved crucial! Exhaustive analysis eventually demonstrated that this was a “cold Neptune” with $q = 8 \times 10^{-5}$.

3.6. 5th+6th Microlensing Planets – Jupiter/Saturn System

On 28 March 2006, the OGLE EEWS noted a tiny 0.1 mag deviation in the previously unremarkable lightcurve of OGLE-2006-BLG-109, but Andrzej was confident enough to issue a public announcement: “Because short-lived, low amplitude anomalies can be a signature of a planetary companion to the lensing star (cf. OGLE-2005-BLG-390) follow-up observations of OGLE-2006-BLG-109 are strongly encouraged!!!” This triggered observations from MDM only a few hours later, which ultimately were important, but the event quickly returned to normal. A few days later, however, it was clearly becoming high-mag, and so drew many observations. Grant Christie caught what seemed like a caustic exit at magnification roughly $A = 500$, 8 days after the first deviation, which definitely raised the excitement level. Within hours, Scott Gaudi had a tentative model. He drew a 6-sided (or 6-cusp) caustic due to a Saturn-mass-ratio planet. The first small bump occurred when the source passed by a cusp. Somehow the source had entered the caustic without being noticed and had just exited. Scott’s trajectory would take the source by another cusp 3 days later, so he predicted another bump at that time. However, reports soon came in from the Wise observatory that the event was rising again, and hours later OGLE observations showed that it was again falling. This new bump, just 12 hours after Grant’s “caustic exit”, seemed to contradict Scott’s 3-day prediction. Nevertheless, after 3 days, Scott’s predicted bump did occur: the Israel/Chile bump had been due to another planet, this one of Jupiter mass-ratio.

It took quite a while to fully decipher this event. The Saturn mass planet was very close to the Einstein ring. In such cases, the size of the caustic scales as $|b - 1|^{-1}$, where b is the planet-star separation in units of the Einstein ring. If $b \sim 1$, then very small changes in b can lead to large changes in the caustic. Thus, the tiny planetary motion during the 8-day interval from the first cusp approach to the caustic exit can lead to big changes in the caustic. On the plus side, this means that if all these features can be properly modeled, one can measure some of the planet-orbit parameters, something no one thought would be possible when microlensing planet searches were initiated. On the minus side, analysis of the lightcurve requires very smart algorithms applied to a supercomputer. Dave Bennett took the lead in this analysis, eventually

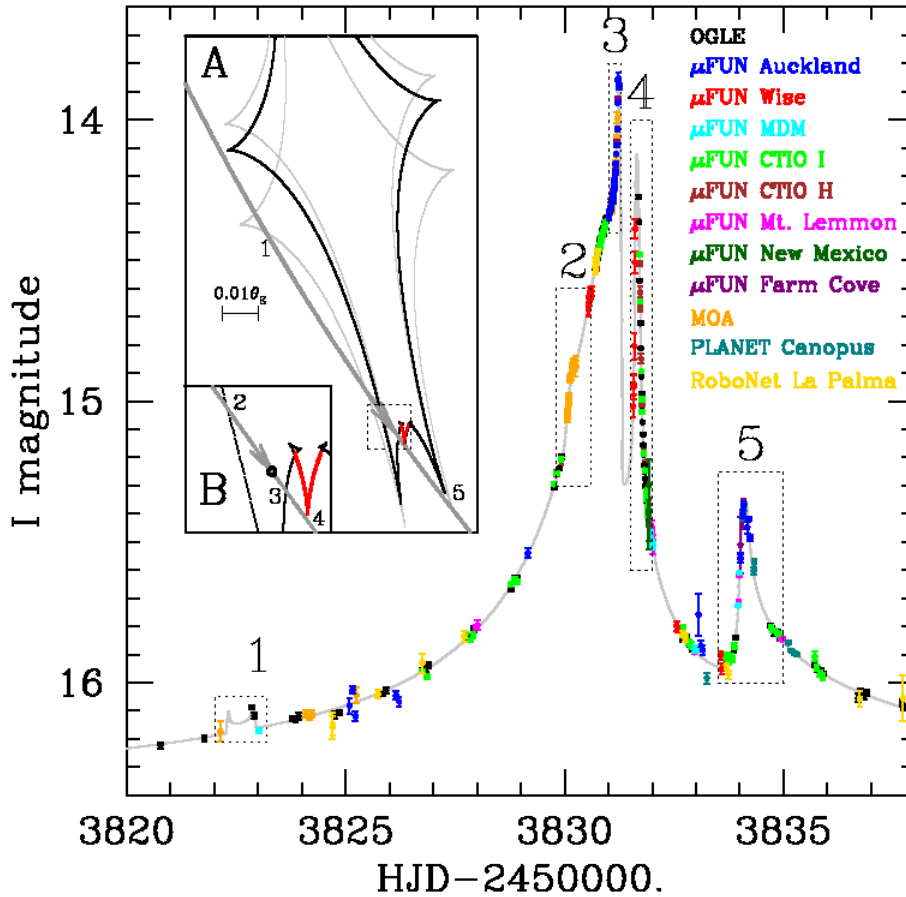


Figure 3. First Jupiter/Saturn analog. This spectacular lightcurve of OGLE-2006-BLG-109 has 5 distinct lightcurve features, which together reveal two planets. Features 1, 2, 3, and 5 come from the black portion of the caustic (*inset A*) due to a Saturn mass-ratio planet very close to the Einstein ring. Feature 4, a sharp “bump” seen from Israel and Chile, cannot be explained by this planet, but it occurs very near the center of the lens geometry, just where perturbations would be expected from other planets that are not near the Einstein ring (*inset B*). This proves to have a Jupiter mass ratio. Because the Saturn is near the Einstein ring, its very small motion leads to dramatic changes in the caustic between the time of Feature 1 (*gray caustic*) and the time of Feature 3 (*black caustic*). Twelve observatories contributed data, notably OGLE (who announced Feature 1 in real time) and New Zealand amateurs Grant Christie and Jennie McCormick, who caught the peak at Feature 3. From Gaudi et al. (2008a).

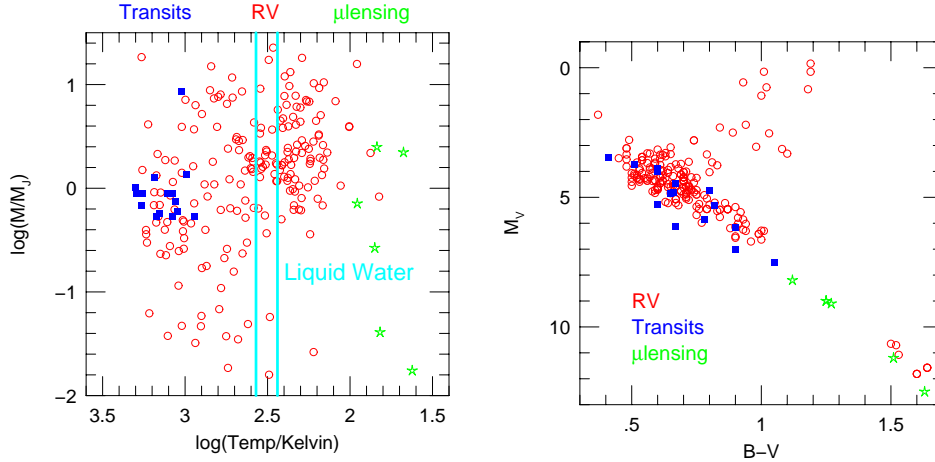


Figure 4. Left: Planet mass vs. equilibrium temperature of planets detected by the Doppler (*red circles*), transit (*blue squares*), and microlensing (*green stars*) techniques, as of June 2007. Microlensing detects planets in the cold, outer regions of their solar systems, where planet formation is expected to be most robust. Right: CMD of the host stars of microlensing planets. Microlensing detects planets without serious selection bias due to host properties. It demonstrates that planet frequency in the outer regions is not strongly dependent on stellar type.

deriving more comprehensive parameters for this system than any other. It is a true Jupiter/Saturn analog, with similar mass ratios and separation ratios as the solar-system gas giants. The equilibrium temperatures of these planets are also similar to Jupiter/Saturn, but a bit cooler (Gaudi et al. 2008a).

It appears that in 2007, microlensers have discovered about 6 more planets, but I have neither the space nor the permission to write about these in detail.

3.7. What Have We Learned About Planets?

Given that microlensing has discovered only a handful of planets, compared to 250+ by other techniques, the scientific payoff has been remarkably high. The difference between community expectations (which were rather dim) and what has actually been achieved is due to two factors.

First, microlensing detections have yielded far more information about the individual star-planet systems than had been thought possible. Originally, it was believed that microlensing detections would return exactly two pieces of information about the system, the planet/star mass ratio q and the planet-star projected separation (in units of the Einstein radius θ_E) b . Only the first quantity was regarded as truly interesting, since the second could not be translated into a physical distance without knowing both θ_E and the distance to the lens D_L . In practice, we have generally been able to make pretty good estimates of the host mass M (and hence the planet mass $m = qM$), as well as θ_E and D_L (and so the projected separation $r_\perp = bD_L\theta_E$). I will discuss exactly how we do this in § 5.2.

Second, microlensing probes a region of parameter space to which other methods are at present largely insensitive, namely the cold regions out past

the snow line, where (at least according standard core-accretion theory) planet formation should be most robust. See Figure 4a. Microlensing is also essentially unbiased by host mass, in sharp contrast to other methods. Hence, as shown by the CMD of planet hosts (Fig. 4b), microlensing detects planets of the most common potential hosts, i.e. late-type stars.

The fact that there are two microlensing detections of cold Neptunes/super-Earths means that these planets are probably extremely common. Gould et al. (2006) estimated that if all stars had planets in this mass range, and in a 0.4 dex annulus bracketing the Einstein ring of the host, then there would have been about 6 detections. In fact there were 2, indicating a rate of roughly 1/3 in this fairly narrow range of radii.

Microlensing sensitivity scales roughly as planet mass. There are 4 Jovian-mass detections and two Neptune-mass detections, and the two classes of planets differ in mass by about 1.5 dex (see Fig. 4a). This indicates that gas giants are of order 7 times less common than ice giants.

Of the 5 planetary hosts, one has two detected planets. As discussed above, these are close analogs of the Jupiter/Saturn pair that dominate the mass in our own solar system. Before planets were discovered, it was generally believed that most solar systems would be like our own. Then with the discovery of the pulsar planets and 51 Peg, weird planets became more fashionable. But the fact is, only microlensing actually has sensitivity to Jupiter/Saturn analogs, so this is the only information we have on how common they are. Microlensing has detected Jovian-mass planets around 3 stars (OGLE-2003-BLG-235/MOA-2003-BLG-53, OGLE-2005-BLG-071, and OGLE-2006-BLG-109). In the first of these, there was a very low probability of detecting a second, Saturn-mass companion had it been there. In the second, there was a modest (roughly 30%) chance. In the third there was an excellent chance (and it was actually detected). This suggests that for systems where there is a Jupiter, it may be highly likely that there is also a Saturn.

Higher-Order Microlensing Effects

Bohdan was fond of pointing out that microlensing is fundamentally such a simple phenomenon that one could predict effects from first principles and then go out and observe these effects in actual events. His favorite example of this was parallax.

4. Microlens Parallaxes

Alcock et al. (1995) made the first microlensing parallax detection but parallax was actually observed in the very first microlensing event observed toward the LMC, MACHO-LMC-5, although no one realized it at the time (Alcock et al. 1997). Indeed no one realized it was the first event at the time: hence its enumeration. MACHO-LMC-5 was weird for other reasons: the CMD position of the apparent source star does not coincide with any LMC population. Gould et al. (1997) had already suggested that this “source” was a foreground M dwarf and that it actually was the lens. After 6 years, MACHO observed this and many other events with *HST* and resolved two stars separated by about 0.1”, a blue

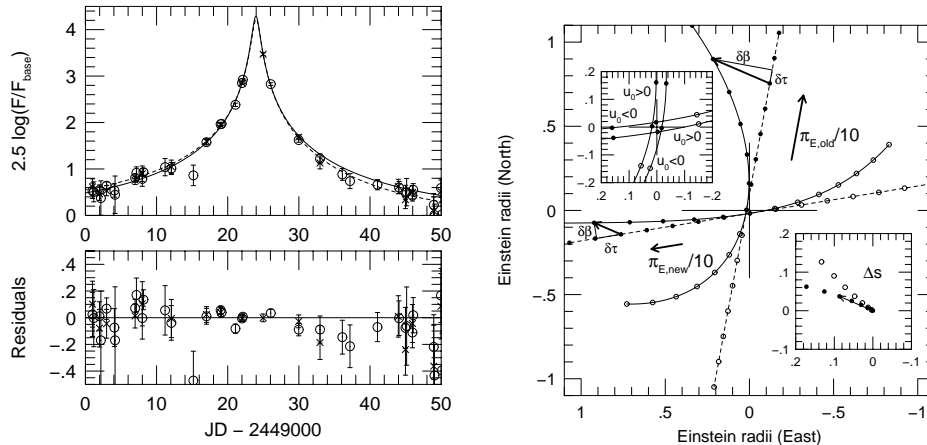


Figure 5. Microlens parallaxes and degeneracies. Left: Lightcurve of MACHO-LMC-5 shows clear asymmetry due to accelerated motion of Earth, falling more rapidly than its rise. Right: 4 possible trajectories of source-lens separation, all curved due to accelerated motion of Earth projected onto the plane of the sky (lower inset). Deviations (from straight lines) are proportional to ΔS (the accelerated displacement of the Earth) and π_E ($=AU/\tilde{r}_E$, the size of the Earth’s orbit relative to the projected Einstein radius). The fact that there are two sets of trajectories with radically different directions and Einstein radii was totally unexpected, but is now understood analytically. From Gould (2004).

LMC star that was clearly the source and a red foreground star, the putative lens (Alcock et al. 2000). But how could one be sure that the red star was not just an unrelated foreground star?

Dave Bennett went back to original lightcurve and noticed the slight asymmetry (Fig. 5a), which led him to fit it for microlens parallax. In analogy to trigonometric parallax, the amplitude of the deviation from rectilinear motion of the source-lens trajectory in microlensing parallax is inversely proportional to the size of what one is trying to measure, i.e., the projected Einstein radius \tilde{r}_E . So just as one writes $\pi = AU/D$ for trig parallax, it is convenient to define the microlens parallax $\pi_E = AU/\tilde{r}_E$. However, in contrast to trig parallaxes, the microlens parallax simultaneously measures the *direction* of lens-source relative motion. So the microlens parallax is actually a vector, $\boldsymbol{\pi}_E$. Dave found that the direction of $\boldsymbol{\pi}_E$ was the same as the vector linking the red and blue stars (Alcock et al. 2001). So the red star *was* the lens, not just a chance interloper!

This result had two important consequences. First, it showed that at least in this case, the lens was not part of a putative dark-matter halo (“MACHO”) population, but was an ordinary disk star. Second, it led to the first mass measurement of an isolated star, which I describe in the next section.

Microlens parallax measurements are relatively rare. Poindexter et al. (2005) found only 22 events (out of about 3000 to that date) for which including parallax effects decreased χ^2 by more than 100. Nevertheless, microlens parallaxes have proved incredibly important, as I discuss in § 5.4.

5. Microlens Masses

From equation (2), one can determine the microlens mass (as well as the lens-source relative parallax), if one can just measure θ_E and \tilde{r}_E (or π_E). As just mentioned, there are very few events for which π_E can be measured. It also turns out that there are very few events for which some “angular ruler” on the plane of the sky permits measurement of θ_E . The number for which the two measurements overlap is minuscule. Nevertheless, microlensing nerds have pursued microlens mass measurements like a holy grail, ultimately with major payoffs. The first microlens mass measurement was EROS-2000-BLG-5 (An et al. 2002), which I discuss in § 5.2..

5.1. First Mass Measurement of an Isolated Star

The second was MACHO-LMC-5. At one level this was trivial: since Alcock et al. (2001) had measured the lens-source separation $\Delta\theta = 0.134''$ after $\Delta t = 6.3$ yrs, they could immediately determine the lens-source relative proper motion $\mu_{\text{rel}} = 21 \text{ mas yr}^{-1}$. Then from the measured Einstein timescale $t_E = 21$ days, they could infer $\theta_E = \mu_{\text{rel}} t_E = 1.2 \text{ mas}$. Unfortunately, when combined with their measurement $\pi_E = 4.2$ (and eq. [2]), this gave them a mass $M = 0.036 M_\odot$ and distance $D_L = 200 \text{ pc}$, which of course would be inconsistent with it being visible in the *HST* image.

Bohdan played a significant role in the resolution of this puzzle. Smith, Mao, & Paczyński (2003) developed an abstract formalism for analyzing parallaxes, which (as referee) I found unexpectedly powerful. They Taylor-expanded the square of the source-lens separation to fourth order in the approximation of uniform acceleration by the Earth. This led them to discover a degeneracy, which changed the trajectory from one side of the Earth to the other (see Fig. 5b, upper inset). Because this degeneracy basically left the magnitude of π_E unchanged, it could not explain the “wrong” mass obtained by Alcock et al. (2001). However, by including jerk in the Taylor expansion, I discovered a second, so-called “jerk-parallax” degeneracy, which did yield a different π_E (see Fig. 5b, main panel). The distance implied by this solution $D_L \sim 550 \text{ pc}$ was later confirmed by Drake et al. (2004) using trig parallax, and the mass estimate $M = 0.097 \pm 0.016 M_\odot$ is consistent with photometric estimates (Gould et al. 2004).

5.2. Multiple Paths to Microlens Mass Measurements

There are basically 4 paths to the microlens parallax π_E : Earth-orbital parallax, trigonometric parallax, Earth-satellite parallax, and terrestrial parallax. All four have been successfully employed. There are also basically 4 angular rulers for measuring θ_E : lens-source proper motion, finite-source effects, image resolution, and centroid displacement. The first of these is measured after the event and the last three during the event. Only the first two have been successfully carried out. As mentioned, microlens mass measurements require one from column A (π_E) and one from column B (θ_E).

For MACHO-LMC-5, θ_E was measured by lens-source proper motion, but this is quite unusual: its proper motion was about 6 times larger than typical lenses toward the bulge, there was a 6-year delay for the second epoch, and *HST* observations were still required to separately resolve the lens and source. By

far the most frequent measurement of θ_E comes from finite-source effects. If the source passes over a caustic, then the lightcurve analysis automatically gives $\rho \equiv \theta_*/\theta_E$, where θ_* is the angular source radius. The dereddened source color gives its surface brightness, and the dereddened magnitude gives its flux, which together yield θ_* . Even in heavily reddened bulge fields, one can deredden the source magnitudes by comparing the position of the source to the clump on an instrumental CMD (e.g., Yoo et al. 2004). This was the method used in the first microlens mass measurement, EROS-2000-BLG-5 (An et al. 2002), which was a binary lens with an extremely well-covered caustic crossing. Such caustic crossings are relatively rare, but what made EROS-2000-BLG-5 really unusual was that it was also an extremely long event, which is what rendered it susceptible to Earth-orbital parallax.

The very largest θ_E could in principle be resolved using interferometry. This would be a good way to confirm black-hole candidates. These have large Einstein rings, so are typically long and so susceptible to Earth-orbital microlens parallaxes. There is an active program to do this at the VLT, but so far it has not been successful. The fourth method will be described in § 5.3.

From equation (2), it is clear that if θ_E is known, then the trig parallax directly yields $\pi_E = \theta_E/\pi_{\text{rel}}$. Hence, Refsdal (1964) already pointed out that microlens masses could be obtained from trig parallaxes and proper motions. More than 40 years later, MACHO-LMC-5 is the only event to which this has been applied in practice (Drake et al. 2004; Gould et al. 2004). Almost all remaining microlens parallaxes come from lightcurve distortions (e.g., Fig. 5a), but there are two exceptions.

The very first idea for microlens parallax was to compare lightcurves obtained from a satellite in solar orbit and the ground (Refsdal 1966). Both the impact parameter and the time of maximum would differ, enabling one to infer both components of π_E . Dong et al. (2007) made such a measurement using the *Spitzer* satellite (see Fig. 6), leading them to conclude that the projected Einstein radius was very large, $\tilde{r}_E \sim 30$ AU. This could be either because the lens was in the SMC or because it was a very massive ($10 M_\odot$) black-hole binary in the Galactic halo. The latter was judged more likely, since the projected velocity $\tilde{v} \equiv \tilde{r}_E/t_E \sim 230 \text{ km s}^{-1}$ is typical for a halo lens but about an order of magnitude smaller than expected for SMC lenses. Still, since there was no measurement θ_E , this conclusion was not absolutely secure.

The reason “solar orbit” is usually required is that typically $\tilde{r}_E \gtrsim 1$ AU, i.e., at least 20,000 times bigger than the Earth. This did not prevent two theorists, Holz & Wald (1996), from pointing out that at least from the standpoint of photon statistics, it would be possible to measure microlens parallaxes from the lightcurve differences from two terrestrial observatories. Amazingly, this has now actually been done as will be discussed elsewhere.

5.3. Future Routine Microlens Mass-Measurements with *SIM*

Given that it has proven so difficult to measure either π_E or θ_E separately, is it possible to *routinely* measure them both together? In fact, this would be possible with the *Space Interferometry Mission (SIM)* (Unwin et al. 2007). *SIM* would be in an Earth-trailing orbit, essentially the same as *Spitzer*, and so could obtain Earth-satellite parallaxes in exactly the same way. But unlike *Spitzer*,

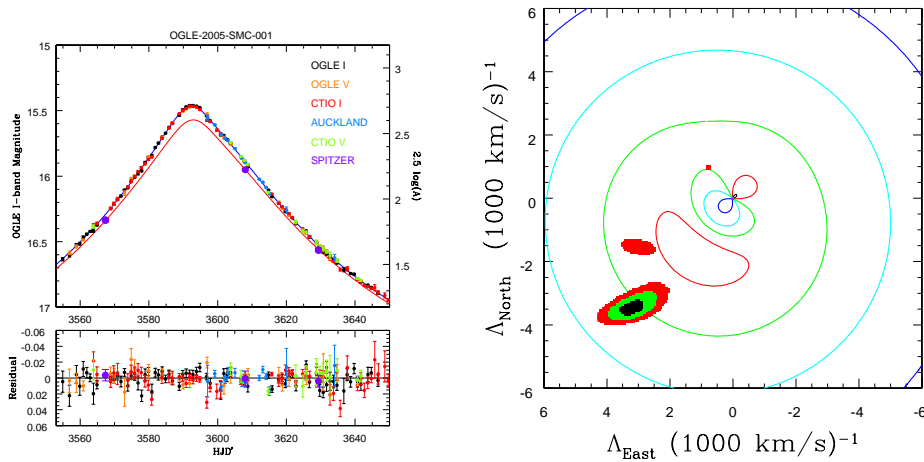


Figure 6. First space-based parallax measurement. Left: OGLE-2005-SMC-001 was observed by the *Spitzer* satellite (*lower curve, purple points*) when it was ~ 0.25 AU from Earth. Offsets in peak time (0.45 days) and peak flux (15%) imply a projected Einstein radius $\tilde{r}_E \sim 30$ AU. Right: Inverse projected velocity $\Lambda \equiv \pi_E t_E / \text{AU}$ of OGLE-2005-SMC-001 (*black, green, red = 1, 2, 3 σ*) is near peak of likelihood contours (*red, green, cyan, blue with factor 5 steps*) expected for halo lenses. That is, the observed $\tilde{v} \equiv \Lambda^{-1} \sim 230 \text{ km s}^{-1}$ is close to typical halo values ($\sim 450 \text{ km s}^{-1}$), but an order of magnitude smaller than typical SMC values (not shown). Adapted from Dong et al. (2007).

it is capable of routinely measuring θ_E as well. Although *SIM* cannot generally resolve the separate images, it can measure the astrometric displacement of the *centroid* of the images relative to the source,

$$\Delta\theta = \frac{A_+ \theta_{I+} + A_- \theta_{I-}}{A_+ + A_-} - \theta_S = \frac{u}{u^2 + 2} \theta_E. \quad (3)$$

This reaches a maximum of $\theta_E / \sqrt{8}$ at $u = \sqrt{2}$. For typical bulge lenses, $\theta_E \sim 300 \mu\text{as}$, so $\Delta\theta_{\text{max}} \sim 100 \mu\text{as}$, a very tiny angle. But *SIM* precision is of order a few μas , meaning that θ_E (and so masses) could be measured to better than 10%. Thus, it would be possible to take a representative census of all objects along the line of sight to the Galactic bulge, whether dark (like black holes) or luminous (like stars).

5.4. Masses for Microlens Planets

As should be clear from the last few sections, an enormous amount of work has gone into developing and applying methods to find θ_E and π_E , yet the few resulting mass measurements have had little direct scientific payoff beyond proving to microlensing nerds that we could do it. In fact, however, there has been a big practical payoff: all 5 planetary hosts described in § 3. have masses and distances that are either measured or strongly constrained. Hence, the 6 planet masses and projected separations are also measured or well-constrained. And it appears that this will also be true for the 6 microlensing planets discovered in 2007. This seems initially implausible, since in general mass measurements

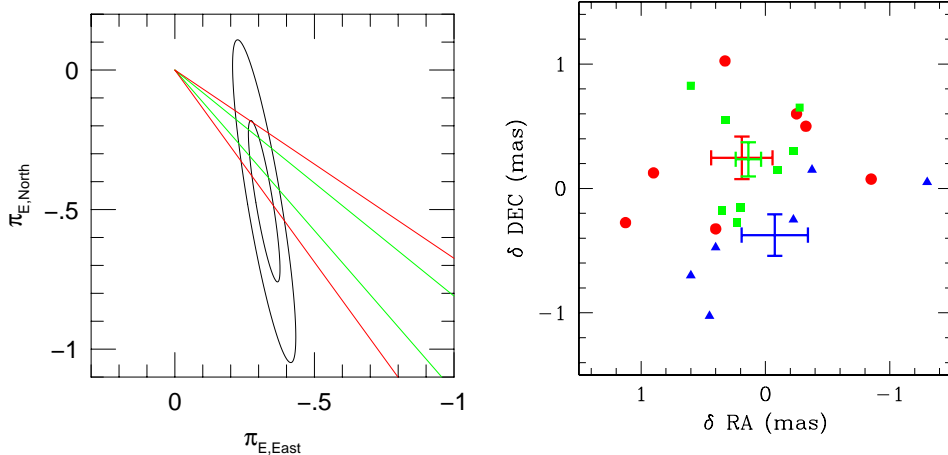


Figure 7. Left: $1\text{-}\sigma$ and $2\text{-}\sigma$ contours for π_E (*black*) of OGLE-2005-BLG-071 (Fig. 2a). Amplitude is microlens parallax π_E and direction is that of lens-source relative motion. Only 1-D is well constrained. Right: Relative source-lens centroids in *B* (*blue*), *V* (*green*), *I* (*red*) of OGLE-2003-BLG-235/MOA-2003-BLG-53 from *HST* images 1.78 years after peak. These yield direction of proper motion (20° north through east). [In a perfect world (without errors) the *V* point would be exactly aligned with the axis connecting the *B* and *I* points, lying slightly closer to the former.] Left (again): A direction measurement from similar observations of OGLE-2005-BLG-071 would resolve its 1-D parallax degeneracy ($1\text{-}\sigma$ [*green*] and $2\text{-}\sigma$ [*red*] lines in left panel).

are so rare. But first, planetary events are “special” in ways that facilitate mass measurements. And second, considerably more effort (both observational and theoretical) is expended by microlensers, once we know the event contains a planet.

The first point is that in sharp contrast to “regular” microlensing events, θ_E is almost routinely measured in planetary events. In ordinary events, the probability that the lens will transit the source (thereby giving rise to measurable finite-source effects) is $\rho = \theta_*/\theta_E$, which is about $\rho \sim 1/500$ for main-sequence sources and typical lenses. But in planetary events, there is hardly any perturbation at all unless the source passes very close to, or right over a caustic, so finite-source effects are almost automatic. To date, all planetary events have them, and they are pronounced in all but OGLE-2005-BLG-071.

Second, due to another selection effect that could hardly have been anticipated, a remarkably high fraction of planetary events have detectable microlens parallax: 2 out of 5. Four of the 5 events were high-mag (due to selection effects described in § 3.2.). These 4 have systematically longer timescales than typical OGLE events. Specifically, they are longer than 79%, 90%, 95%, and 97% of them, respectively. And long events display measurable parallaxes much more often, simply because the Earth’s motion deviates from a straight line during the event as the square of the Einstein timescale. Why are planets found preferentially in long events? One definite reason is that, by definition, long events unfold more slowly, which increases the chance that their high-mag character will be recognized in time to initiate the dense monitoring required to find planets.

A second possible reason is that the planets we are finding seem to be orbiting foreground disk stars, rather than bulge stars, and disk-lens events tend to be longer than bulge-lens events. At this point, we cannot tell which way this selection pressure is working (i.e., if most planets are in the disk, which would bias us toward the intrinsically longer disk events, or if the long events being better observed is biasing us toward monitoring events caused by disk stars) or even if the effect is real, but it is a possibility to keep in mind.

Whatever the exact cause, two events (OGLE-2006-BLG-109 and OGLE-2005-BLG-071) have measurable parallaxes. The first of these is quite good, but the second is rather crude: its π_E 1- σ error-ellipse axes are (0.6×0.06) . See Figure 7a. Under normal circumstances, we would not call this a “measurement” at all, or rather, we would call it a “one-dimensional parallax” and move on. The origin of such 1-D parallaxes is easily seen from Figure 2a: the lightcurve is asymmetric, being above the model on the rise and below it on the fall. This effect is caused by the uniform component of the Earth’s acceleration toward the projected position of the Sun at the peak of the event, and so very well constrains $\pi_{E,\parallel}$, the component of π_E in this direction. Only longer, or much more precisely photometered, events reveal the much subtler effects from motion in the direction perpendicular to the Sun.

While the OGLE-2005-BLG-071 parallax “information” is rather ambiguous on its own, it could be transformed into a genuine microlens parallax if, somehow, the direction of lens-source motion (and so of π_E) could be independently determined. And this brings us to yet another type of information that is not usually available for normal events: high-resolution post-event imaging. We already saw that the source and lens were separately resolved 6 years after peak for MACHO-LMC-5 (§ 5.1.). That was only possible because the relative proper motion was exceptionally fast and the observers were ready to wait an exceptionally long time. But much smaller source-lens relative displacements can be detected by taking advantage of the fact that the source and lens generally have different colors. This means that the *centroids* of B and I light will be displaced from one another as the source and lens separate, long before the two stars are separately resolved. The amplitude of the centroid displacement is the product of the lens-source displacement and a function of the B and I mags of the two stars. Figure 7b shows an example of this using post-event *HST* images of OGLE-2003-BLG-235/MOA-2003-BLG-53. In this case, the source-lens displacement was known (from finite-source effects), so the centroid offset yielded the color-function, which was used (together with stellar color-mag relations and the source flux as determined from the microlensing fit) to estimate the lens mass. However, similar measurements made several years after the peak of OGLE-2005-BLG-071 could be applied to reverse effect. That is, to the extent that the color-function is known (which it approximately is in this case from *HST* images during the event), the centroid displacement would give the lens-source displacement (and so μ_{rel} and hence $\theta_E = \mu_{\text{rel}}t_E$). And, more importantly in the present context, *whether or not the color function is known*, the centroid color displacement gives the *direction* of μ_{rel} , which is the same as the direction of π_E . Figure 7a shows the result of a hypothetical future centroid-offset measurement for OGLE-2005-BLG-071. This offset “picks out” a narrow subset of the parallax solutions, transforming the 1-D parallax derived from the lightcurve into a 2-D parallax.

While no such late-time astrometry of OGLE-2005-BLG-071 has yet been obtained, Subo Dong (in preparation) has made an incredibly detailed investigation of a variety of higher-order effects, including the 1-D parallax just described, constraints on the proper motion from finite-source effects and from event and post-event *HST* imaging, limits on the presence of third bodies from the lack of lightcurve distortions, and others. Together these imply that the lens star is probably a high-velocity, low-metallicity (i.e., thick disk) M dwarf, which would be rather unexpected for a planetary host. Late-time astrometry would confirm (or contradict) these tentative conclusions.

In brief, by taking advantage of intensive observations during the event, taking carefully chosen high-resolution images during and after the event, combining all available data, and performing systematic cross-checks among them, it is often possible to measure masses and distances accurate to 20% or better. Even when the only pieces of information are θ_E and t_E , it is still possible to combine these with priors for the lens and source distances and velocities to derive a statistical estimate of the lens mass. This was the approach taken for the cold super-Earth OGLE-2005-BLG-390 (§ 3.4.) and the cold Neptune and OGLE-2005-BLG-169 (§ 3.5.).

6. Binary Lens Revolution

MACHO-97-41 was a curious event. It showed a short, 3-day bump and then seemed to return to normal. A week later it began rising sharply, briefly spiking to magnification $A = 40$ before returning to baseline. See Figure 8a. The second bump is easily fit as the central caustic of a close-binary lens (i.e., with both components inside the Einstein ring). Such close binaries always have two small outlying caustics in addition to the central caustic, which would seem to explain the first bump. The trouble was, the predicted position of this small caustic had the wrong distance from the central caustic to account for the timing of the first bump and the wrong angular position to be intersected by the source trajectory (*red* caustic in Fig. 8b) However, both effects are easily explained by “binary revolution”. To the extent that components move farther apart, the outlying caustic will move closer to the central caustic. And to the extent that they rotate on the sky, the angular position of the caustic will change (*cyan* caustic in Fig. 8b). Hence, the very peculiar geometry of this event permits measurement of the two instantaneous components of the binary internal motion on the plane of the sky.

This example immediately raises two important questions. First, how do we know that this very complicated model, which predicts the incredibly elaborate (and largely unobserved) lightcurve seen in Figure 8a, is actually correct? And second, who (besides microlensing nerds) cares?

As it happens, in this case, two completely independent groups observed this event and the model shown (based only on the data shown) predicts the second data set almost perfectly. This is a pretty important test of the robustness of microlens models of complex lightcurves with higher order effects.

As to the second question, at least for 10 years the answer was “no one”.

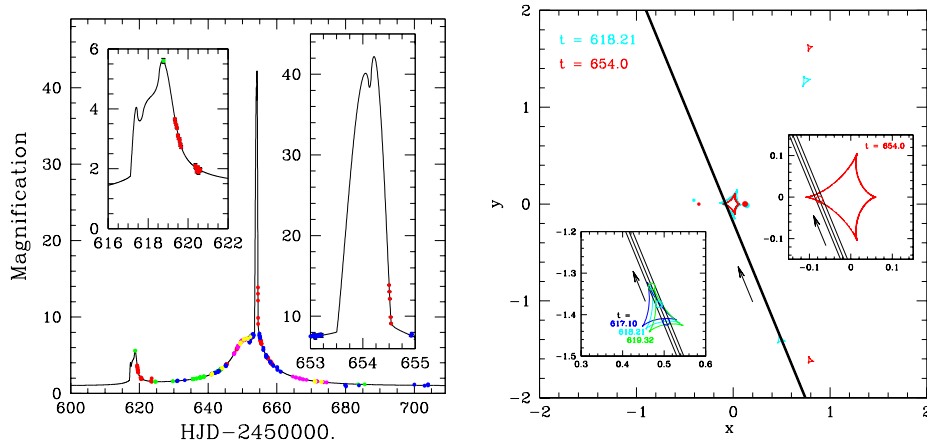


Figure 8. Binary revolution in MACHO-97-41. Left: PLANET lightcurve and model (Albrow et al. 2000). Two bumps are due to outlying and central caustics of close binary, respectively. “Wild” features of model without data points are confirmed by independent data set (Bennett et al. 1999) [not shown]. Right: In static model (*red caustics*) trajectory determined from central caustic does not pass through outlying caustic. Rotating model (*cyan caustics*) rotates and moves inward the position of the outlying caustic so that it matches data.

6.1. Planetary Lens Revolution

Despite early predictions that a Jupiter-mass planet would generate 1-day deviations, 3 of the 5 planetary events have had 3–12 day perturbations. The fundamental reason for this is that the probability of detecting a planet is proportional to the size of the caustic, so the relatively rare planets that are close to the Einstein ring (and so have large caustics $\propto 1/|b-1|$) have enhanced probability of detection and also proportionately longer planetary perturbations.

The durations of these perturbations are still very short compared to the typical orbital periods (several years), so one would not at first sight expect any noticeable change in the caustic during the perturbation. But the very fact that the caustic size is $\propto 1/|b-1|$, means that for $b \sim 1$, small changes in b lead to large changes in caustic size. Similar leverage applies to angular motions. In the case of OGLE-2006-BLG-109, $b = 1.04$. Hence, a change in b of less than 0.5% during the 8-day interval between the first cusp crossing and the peak, would lead to a 10% change in the caustic size. Far from being almost too subtle to measure, this effect was so pronounced that it was initially impossible to fit the first cusp crossing at all, until eventually revolution was included in the fit.

While the two-planet system OGLE-2006-BLG-109Lb,c enabled the most dramatic measurement of internal planetary motions, OGLE-2005-BLG-071 also shows evidence of revolution, despite its very short, 3-day perturbation. And, for the reasons just given, we can expect revolution to be measurable in a significant fraction of central-caustic events in the future.

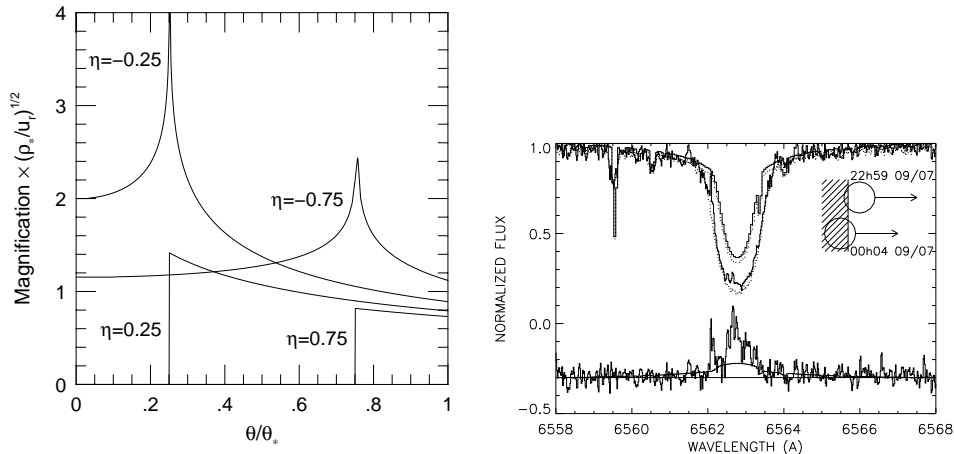


Figure 9. Left: Magnification profiles of different stages of a caustic exit. For example, when the source center is $\eta = 0.75$ source radii outside the caustic, caustic magnifies the outer 25% of the source about equally, and leaves the rest of the source essentially unmagnified. From Castro et al. (2001). Right: $H\alpha$ profiles of OGLE-2002-BUL-069 when it was just starting and just finishing its exit (see inset). The latter shows an emission bump, probably due to the chromosphere (Cassan et al. 2004).

7. Stellar Atmospheres

Microensing has proven to be a powerful tool to study stellar atmospheres in two distinct ways. First, microlens caustics can resolve the surfaces of stars better than any other technique, with the possible exception of transiting planets. Second, microlenses can act as a huge magnifying glass to obtain spectra of stars that would be prohibitively expensive to observe under ordinary circumstances.

7.1. Limb Darkening

Figure 9a shows the magnification due to a caustic as a source exits a so-called “fold caustic” (i.e. a square-root singularity). The surface is assumed to be radially symmetric (no spots). Consider first the “ $\eta = 0.75$ ” curve, which describes the magnification profile when the center of the star is 3/4 of the way past the caustic. Of course, only the outer 25% of the star is magnified by the caustic at all. Figure 9a shows that all radii are magnified about equally. A photometric series from $\eta = 0$ to $\eta = 1$ would give a set of box-car convolutions with the radial profile, permitting straightforward deconvolution of the intrinsic profile. The $\eta < 0$ profiles are more complicated, but do add some additional information. (Of course, in addition to the caustic magnification, there is the underlying non-caustic magnification, which must be taken into account in the process. But this is smooth and also straightforward to model.) The most spectacular application of this technique was carried out by Fields et al. (2003) using PLANET data on EROS-2005-BLG-5, which had a K-giant source. This provided by far the most detailed profile of any star except the Sun and was also the first (non-solar) confrontation of limb-darkening models with data. How did the models do? They look broadly similar to the data but do not agree in detail. In par-

ticular, when K-giant profiles are plotted for a range of temperatures near that of EROS-2005-BLG-5, they share a “fixed point” with each other and also with the observed profile of the Sun. But the deconvolved microlensing profile does not share this “fixed point”. Hence, the K-giant models appear to extrapolate from some physics in the Sun that is not actually shared by K giants.

So far, no atmosphere modelers have risen to this challenge.

7.2. Chromospheric Spectra

Two groups obtained spectra of EROS-2000-BLG-5 in an effort to resolve the source surface simultaneously in spatial and spectral dimensions (Castro et al. 2001; Albrow et al. 2001). In particular, Albrow et al. (2001) found about 20% less $H\alpha$ absorption when, based on the photometric lightcurve, the source had nearly exited the caustic. Afonso et al. (2001) argued that too little of the source was under the caustic to have such a large effect, and the only plausible explanation was that the chromosphere (which was strongly magnified during this observation) has very strong $H\alpha$ emission. Unfortunately, this conjecture could not be tested in this event because the Albrow et al. (2001) spectra were low-resolution, rendering impossible any identification of separate components to the line.

However, Cassan et al. (2004) did obtain a high-resolution spectrum of another K giant, OGLE-2002-BUL-069, just as it was ending its exit from a caustic, as well as a comparison spectrum when it was just beginning its exit. See Figure 9b. The second spectrum shows a distinct “bump” in the $H\alpha$ trough, confirming strong chromospheric emission.

7.3. Microlenses as Magnifying Glasses

Minniti et al. (1998) published spectroscopic observations of microlensed bulge source under the provocative title “Using Keck I as a 15m Diameter Telescope”. The idea was that the source was already magnified by a factor of 2.25, so these observations were equivalent to using a 15m telescope at the same exposure time. Now, events remain magnified by a factor 2 for a week or two, so with some modest planning one could arrange to cut down on long exposures considerably this way. But when planetary microlenses began concentrating on high-mag events, much more dramatic improvements became possible.

The first example of this occurred in a quite unplanned way. Avishay Gal-Yam was at Keck when (as a member of μ FUN) he received a flurry of emails urgently requesting *photometric* observations of OGLE-2006-BLG-265, which eventually reached magnification $A = 230$. He decided to get a 15 minute spectrum (at $A = 130$, it turned out), thus using Keck as a 115m telescope on this $I = 19.4$ star! This was by far the best spectrum of a bulge dwarf to that time. See Figure 10a. Once again, the initiative of the observer proved crucial. Johnson et al. (2007) analyzed this spectrum and found a G-dwarf with $[\text{Fe}/\text{H}] = 0.55$, one of the most metal rich stars yet observed. See Figure 10b.

These results inspired a somewhat more systematic effort to obtain such spectra as part of the “normal” frenetic activity that surrounds high-mag events. Scott Gaudi obtained another spectrum a few weeks later of MOA-2006-BLG-099 (Johnson et al. 2008), and another substantially higher S/N spectrum of OGLE-2007-BLG-349 was obtained by Judy Cohen the next year (Cohen et al.

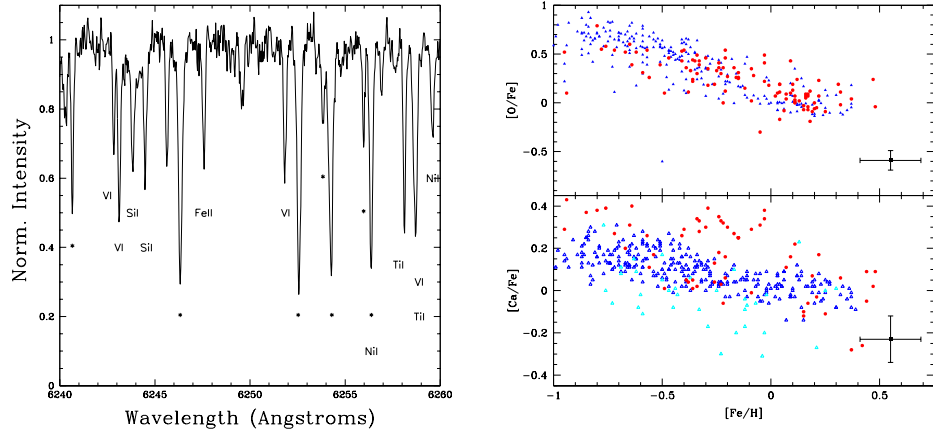


Figure 10. Using Keck as a 115m telescope. Left: 15 minute Keck spectrum of OGLE-2006-BLG-265 when it was magnified by $A = 130$. Right: Abundance measurements derived by Johnson et al. (2007). The first bulge dwarf with a very high quality spectrum proves to be one of the most metal-rich bulge stars.

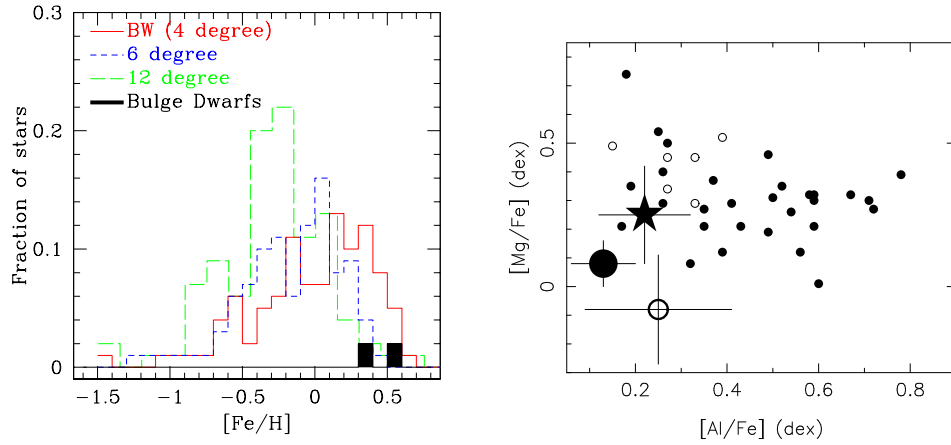


Figure 11. Left: Iron abundances of first two highly-magnified bulge dwarfs (black), OGLE-2006-BLG-265 (see Fig. 10) and MOA-2006-BLG-099 (Johnson et al. 2008) compared to those of bulge giants (histograms). A third dwarf, OGLE-2007-BLG-349 (Cohen et al. 2008), also has $[\text{Fe}/\text{H}] = +0.5$, making the dwarf and giant distributions inconsistent at 4×10^{-5} . Right: $[\text{Mg}/\text{Fe}]$ and $[\text{Al}/\text{Fe}]$ ratios of the three highly magnified dwarfs (large symbols) compared to those of bulge giants (Cohen et al. 2008).

2008). These two dwarfs are also iron rich, and a KS test (probability 4×10^{-5}) shows that these metallicities are not drawn from the same distribution found for giants. See Figure 11. The most likely explanation is that metal-rich dwarfs blow off their envelopes before they can become evolved giants, so giant stars are not representative of the underlying population.

8. Coming Full Circle: Domestic Microlensing Event

Einstein (1936) famously dismissed microlensing in the very paper he introduced it: “Some time ago R.W. Mandl paid me a visit and asked me to publish the results of a little calculation, which I had made at his request . . . there is no great chance of observing this phenomenon.” In fact, Rudi Mandl, a Czech electrical engineer, after perhaps failing to gain Einstein’s attention by mail, obtained “a small sum of money” from the Science Service to come to Princeton to pester Einstein in person. Einstein already knew, or thought he knew, that microlensing was unobservable because he had already worked out the magnification and cross section in 1912 (Renn et al. 1997). Hence, as his private remarks to the editor of *Science* reveal, he was actually far more dismissive of this idea than even his article indicated: “Let me also thank you for your cooperation with the little publication, which Mister Mandl squeezed out of me. It is of little value, but it makes the poor guy happy.”

Why was Einstein so down on microlensing? One reason appears sound. In 1936, photographic catalogs went to about $V = 12$, about the limit of the Tycho-II catalog. So there would have been of order 2 million stars, the giants among which would typically be at about 2 kpc. It is straightforward to work out that the optical depth for these stars is $\tau \sim 10^{-8}$ and that they have an event rate $\Gamma \sim 10^{-7} \text{ yr}^{-1}$. Hence, even if all these stars were monitored continually with a precision much better than 0.3 mag (a complete impossibility in Einstein’s day), there would be only 1 event every 10 years.

In fact, it is unlikely that Einstein ever did this calculation. For one thing, he evaluates what we would call the Einstein radius as “a few light seconds”, whereas it is more like a few hundred light seconds, meaning that he was discouraged from doing a detailed calculation before he got to this stage. But for another, one gains the definite impression from his article that he was thinking of microlensing as a static, not dynamic phenomenon. He says (in our notation) that u “must be small compared to [unity], [to produce] an appreciable increase of the apparent brightness” of the source. This implies that he considered the phenomenon to be unobservable unless the magnification were very high, much greater than unity. Since low amplitude variables were known in Einstein’s day, this must mean that he was not thinking about *microlensing events*, but rather thought that for a microlensed star to be noticed, it would have to be anomalously bright (e.g., for its color). And recognizing microlensing events by this path would indeed be extraordinarily difficult, even today. It appears that it was Russell (1937) who thought of the idea of microlensing *events*, albeit in a context rather different from the ones we observe today. So, while the term “Einstein ring” does reflect the real history of this subject, perhaps it would have been more appropriate to refer to the “Russell timescale”.

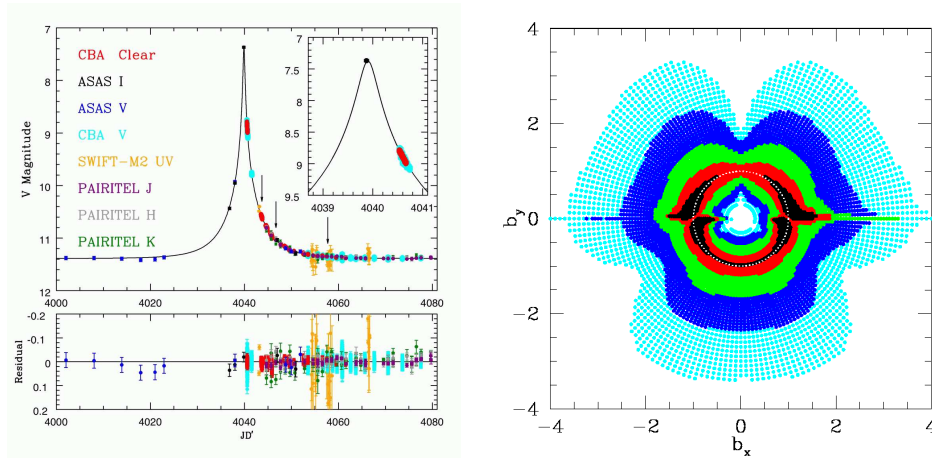


Figure 12. Domestic Microlensing Event. Left: Light curve of microlensing event of a nearby $V = 11$ A star, discovered by amateur Akihiko Tago and monitored on its fall by Joe Patterson’s Center for Backyard Astrophysics. Grzegorz Pojmański’s ASAS all-sky monitoring, recovered after the event, proved crucial in demonstrating that the lightcurve is symmetric, and so is almost certainly microlensing. Right: Planet sensitivity of this event assuming that ASAS observations had been analyzed in time to issue a microlensing alert, thus allowing the event to be monitored intensively over peak. Contours vary from $q = 10^{-5}$ (black) to $q = 10^{-3}$ (cyan). Planet-star separation is in units of the Einstein radius. From Gaudi et al. (2008b)

A recent observation of a “domestic microlensing event” calls into question Einstein’s dismissal, even judged on its own terms. And here again, Bohdan played a role, albeit indirect. Akihiko Tago, a Japanese amateur who has been scanning the sky for 40 years for novae and comets, noticed that a $V = 11$ A star had suddenly brightened by 4 magnitudes. He issued an alert which was picked up by Joe Patterson’s Center for Backyard Astrophysics (CBA), a network of amateurs and professionals dedicated to variable phenomena. After Joe had ruled out all other explanations, he concluded that the lightcurve could only be microlensing and sent the data to Scott Gaudi and me. I promptly told him it could not be microlensing for two reasons. First, by the argument that Einstein either made, or might have made, such events are too rare. Indeed the above calculation was for the rate of events with impact parameters $u_0 < 1$, i.e., all source trajectories that cross any part of the Einstein ring. However, this event, if it indeed were microlensing, would have been magnified 40 times and so would have been 40 times rarer. But second, even combining the discovery data and the CBA data, only the falling part of the lightcurve was available. It is well known that the falling lightcurves of novae and other eruptive variables can look like microlensing, but are easily discriminated by the asymmetry between their rise and fall. Even if this A star was not some known type of variable, without a rising lightcurve, it was more likely to be an unknown variable than microlensing, although lack of Xray emission and emission features in the optical spectrum did tend to weigh against an eruptive variable.

Enter Grzegorz Pojmański and his ASAS project, which as he relates in this volume, was nurtured and encouraged by Bohdan. ASAS was already functioning in the south, but had only begun test observations in the north. When contacted, Pojmański found that ASAS observations covered both the rise and fall of the event, and indeed one observation right at peak. See Figure 12a.

These proved two things. First the event is symmetric and so almost certainly is microlensing (Fukui et al. 2007; Gaudi et al. 2008b). Second, it could not have been recognized as microlensing just based on observations (by amateurs or professionals) that could have been made in Einstein's day. Automated observations of large parts of the sky are required.

While microlensing events of stars at 1 kpc probably really are quite rare, relatively nearby events at 4 kpc occur several times per year. At the end of his life, Bohdan was thinking about next generation wide-field surveys that could detect these. If detected and publicized before peak, such events could open a new avenue of planet detection. Figure 12b shows the sensitivity to planets (including Earth-mass planets *black*) of hypothetical observations of the event at left, assuming that it had been alerted in time to densely monitor the peak.

9. Conclusions

The microlensing surveys that began in the 1990s are directly traceable to Bohdan's influence, inspiring the Magellanic Cloud surveys with his 1986 article and directly helping to initiate and guide OGLE. As advocated by Paczyński (1986), these searches began by looking for dark matter, but Bohdan began immediately to push microlensing in new directions, particularly planets and Galactic structure. Two decades later, microlensing has become an incredibly powerful tool and an incredibly rich subject.

Acknowledgments. I thank Rich Gott for valuable insights into the early history of microlensing, and Scott Gaudi for a careful review of the manuscript. This work was supported in part by grant AST-042758 from the NSF.

References

- Afonso, C. et al. 2001, A&A, 378, 1014
- Albrow, M. et al. 1998, ApJ, 509, 687
- Albrow, M. et al. 2000, ApJ, 534, 894
- Albrow, M. et al. 2001, ApJ, 550, L173
- Alcock, C. et al. 1995, ApJ, 454, L125
- Alcock, C. et al. 1997, ApJ, 491, 436
- Alcock, C. et al. 2000, ApJ, 552, 582
- Alcock, C., et al. 2001, Nature, 414, 617
- An, J.H., et al. 2002, ApJ, 572, 521
- Beaulieu, J.-P. et al. 2005, Nature, 439, 437
- Bennett, D.P., et al. 1999, Nature, 402, 57
- Bennett, D.P., Anderson, J., Bond, I.A., Udalski, A., & Gould, A. 2006, ApJ, 647, L171
- Bond, I.A., et al. 2004, ApJ, 606, L155
- Drake, A.J., Cook, K.H., & Keller, S.C. 2004, ApJ, 607, L29
- Cassan, A. et al. 2004, A&A, 419, L1
- Castro, S.M., Pogge, R.W., Rich, R.M., DePoy, D.L., & Gould, A. 2001 ApJ, 548 L197

- Cohen, J.G., Huang, W., Udalski, A., Gould, A., Johnson, J. 2008, ApJ, submitted
arXiv:0801.3264
- Dong, S., et al. 2006, ApJ, 642, 842
- Dong, S., et al. 2007, ApJ, 664, 862
- Einstein, A. 1936, Science, 84, 506
- Fields, D. et al. 2003, ApJ, 596, 1305
- Fukui, A. et al. 2007, ApJ, 670,423
- Gaudi, B.S. 2008a, Science, in press
- Gaudi, B.S. 2008b, ApJ, in press, astro-ph/0703125
- Gould, A. 2000, ApJ, 542, 785
- Gould, A. 2004, ApJ, 606, 319
- Gould, A., Bennett, D.P., & Alves, D.R. 2004, ApJ, 614, 404
- Gould, A., & Loeb, A. 1992, ApJ, 396, 104
- Gould, A. Bahcall, J.N., Flynn, C. 1997, ApJ, 482, 913
- Gould, A., et al. 2006, ApJ, 644, L37
- Griest, K. & Safizadeh, N. 1998, ApJ, 500, 37
- Holz, D.E. & Wald, R.M. 1996, ApJ, 471, 64
- Jaroznyński, M. & Paczyński, B. 2002, Acta Astron. 2002, 52, 361
- Johnson, J.A., Gal-Yam, A., Leonard, D.C., Simon, J.D., Udalski, A., & Gould, A.
2007, ApJ, 655, L33
- Johnson, J.A., Gaudi, B.S., Sumi, T., Bond, I.A. & Gould, A. 2008, ApJ, submitted,
arXiv:0801.2159
- Mao, S. & Paczyński, B. 1991, ApJ, 374, L37
- Minniti, D., Vandehi, T., Cook, K.H., Griest, K., & Alcock, C. 1998, ApJ, 499, L175
- Paczynski, B. 1986, ApJ, 304, 1
- Paczynski, B. 1991, ApJ, 371, L63
- Poindexter, S., et al. 2005, ApJ, 633, 914
- Rattenbury, N. J., Bond, I. A., Skuljan, J., & Yock, P. C. M. 2002, MNRAS,
- Refsdal, S. 1964, MNRAS, 128, 295
- Refsdal, S. 1966, MNRAS, 134, 315
- Renn, J., Sauer, T., & Stachel, J. 1997, Science, 275, 184
- Russell, H.N. 1937, Scientific American, 156, 76
- Smith, M.C., Mao, S., & Paczyński, B. 2003, MNRAS, 339, 925
- Udalski, A., et al. 2005, ApJ, 628, L109
- Unwin, S.C. et al. 2007, PASP, in press, (astro-ph/0708.3953)
- Yoo, J., et al. 2004, ApJ, 603, 139